CHAPTER 7

RESULTS AND DISCUSSION

In this chapter, the proposed analysis method for the stability and bifurcation analysis of crack patterns will be tested. The method employs the smeared crack finite element analysis with the mixed formulation for investigating stability of equilibrium paths and locating bifurcation points. In addition, the method also employs different search algorithms to obtain the true equilibrium path when bifurcation occurs. In this chapter, the following problems are considered, i.e.,

- A direct tension problem of a plain concrete bar with notches on one edge using four-noded quadrilateral elements,
- A four-point bending problem of plain concrete using four-noded quadrilateral elements,
- A four-point bending problem of steel-fiber-reinforced concrete using four-noded quadrilateral elements.

7.1 A Direct Tension Problem of a Plain Concrete Bar with Notches on One Edge Using Four-Noded Quadrilateral Elements

Consider a numerical direct tension test of a bar with notches as shown in Fig. 7.1. The figure shows the details of the geometry of the specimen and also the material properties used in this problem. The reason why the notches are introduced to

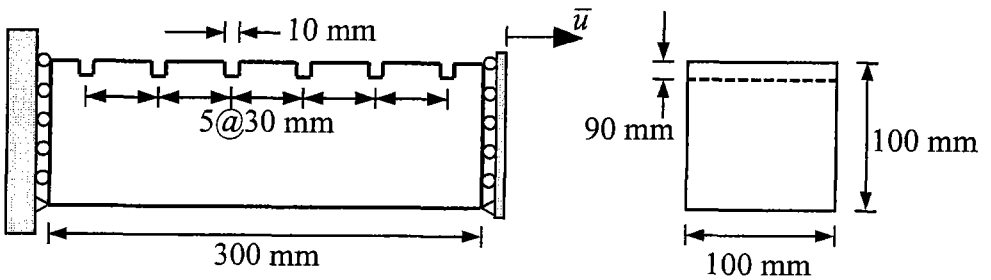

(a) Specimen geometry

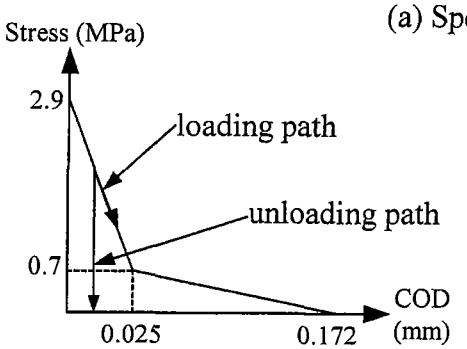

(b) Tension-softening curve

Young's modulus = 27,500 MPa
Poison's ratio = 0.2

(c) Elastic properties

Fig. 7.1 Direct tension test of a bar with notches on one edge

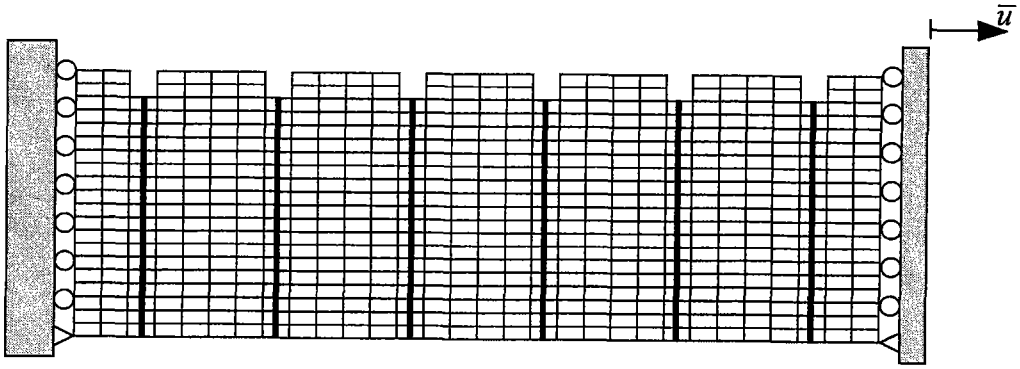

Fig. 7.2 Finite element mesh for the direct tension test with notches

the bar on one side is to pre-specify the crack paths and to, at the same time, study the effect of the unsymmetric crack growth. For this problem, four-noded quadrilateral plane stress elements are used (see Fig. 7.2). In the mesh, there are 651 nodes and 588 elements. Each element can accommodate one crack. Since the alignment of each crack is vertical and the elements are perfect rectangles, the characteristic length of each crack is equal to the horizontal dimension of the element (width of an element). The conventional bilinear shape function is used for the displacement and local crack strain interpolations. Fig. 7.2 also shows the paths where cracks are allowed to propagate.

The loading is performed by increasing the controlled horizontal displacement of the right and of the bar. Since, there are totally six crack paths that are allowed to occur, the selection of the minimum total potential energy will be based on the exhaustive search in which the exact minimum total potential energy with respect to the interpolations used can be obtained. Fig. 7.3a shows the load-controlled displacement response of this problem. The first cracked elements will be initiated when the load reaches approximately 65 percent of the peak load (see Fig. 7.3b). After that, they continue to propagate in a stable manner until the peak load is nearly reached. At about the peak load, the crack pattern becomes unstable and localization of cracks takes place (see Fig. 7.3c-e). At the peak load, there are only two paths of cracks that continue to open (see Fig. 7.3e). In the post-peak region, the load is decreased rapidly as the cracks in the two major crack paths open wider.

If the localization of cracks is not considered in this problem, after the initiation of the first cracks, all cracks will continue to open and there will be no unloading cracks. The obtained response will be completely different from the correct response which considers the localization. The instability of this crack pattern with two opening-crack paths occurs finally and the cracks localize into one major crack. The final crack pattern is shown in Fig. 7.3f.

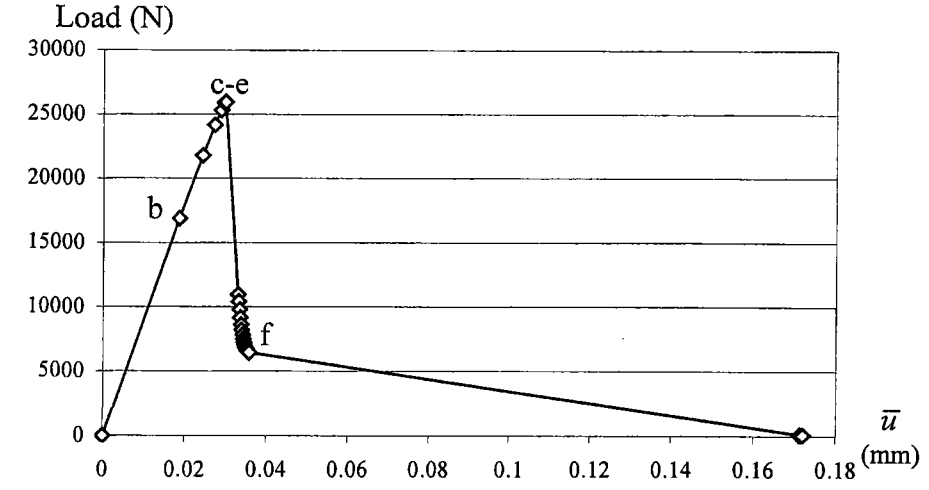

(a) Load-controlled displacement response

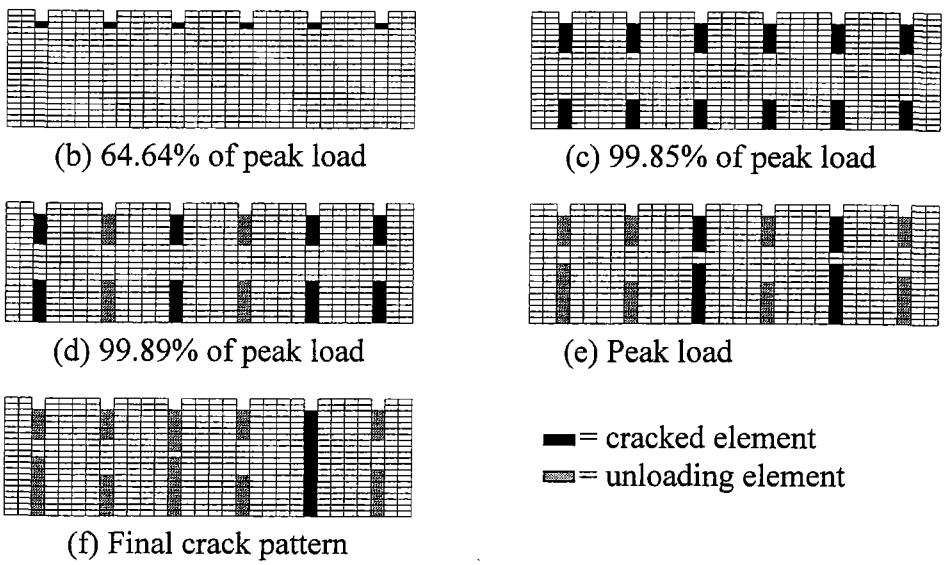

(b) 64.64% of peak load

(c) 99.85% of peak load

(d) 99.89% of peak load

(e) Peak load

= cracked element

= unloading element

(f) Final crack pattern

Fig. 7.3 Load-controlled displacement response and crack patterns

7.2 A Four-Point Bending problem of Plain Concrete Using Four-Noded Quadrilateral Elements

In this problem, the classical four-point bending beam test of plain concrete shown in Fig. 7.4a is investigated. This problem is one of the standard problems for testing analysis methods for cracking localization. The reason is that, under the test configuration, the axial stress at the bottom fiber of the beam in the middle span will be quite uniform. This will subsequently result in many cracks distributed uniformly along the bottom of the beam in the middle span. These cracks will, at the beginning, grow but finally only major cracks will continue to grow while the others stop growing and start to unload. Having many cracks before the localization makes the localization analysis rather difficult.

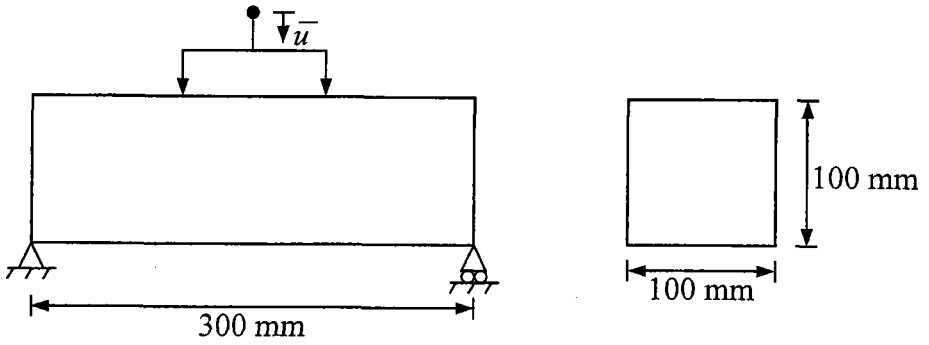

(a) Specimen geometry

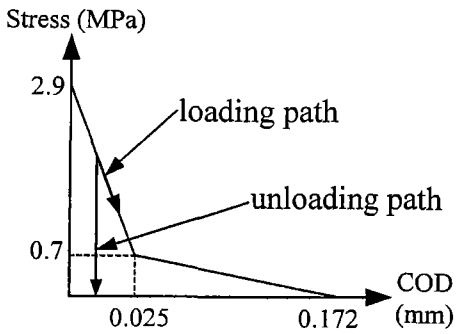

(b) Tension-softening curve

Young's modulus = 27,500 MPa
Poison's ratio = 0.2

(c) Elastic properties

Fig. 7.4 Four-point bending problem of plain concrete

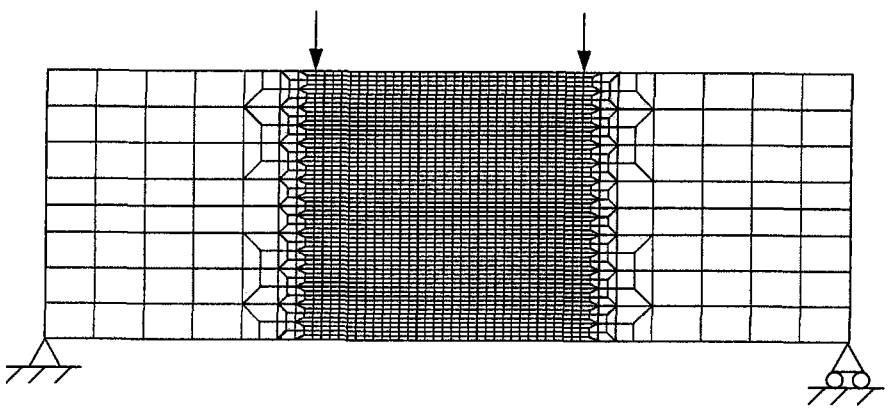

Fig. 7.5 Finite element mesh for four-point bending problem

The dimensions of the specimen in this problem are 300×100×100 mm. Controlled displacements are applied at the top of the beam, 100 mm from both ends. Young's modulus and Poison's ratio used are 27.5 GPa and 0.2, respectively. Unit weight of the material is 2,300 kg/m^3. The tension-softening curve used is shown in Fig. 7.4b. In the analysis, four-noded quadrilateral elements are employed. The conventional bilinear shape function is used for the displacement and local crack strain interpolations. A finite element mesh used in this analysis consists of 2,232 elements and 2,288 nodes (see Fig. 7.5). Note that each element can accommodate one crack.

For this problem, it can be reasonably assumed that all crack paths are straight. To simplify the problem, cracks will be allowed to occur only on the pre-specified

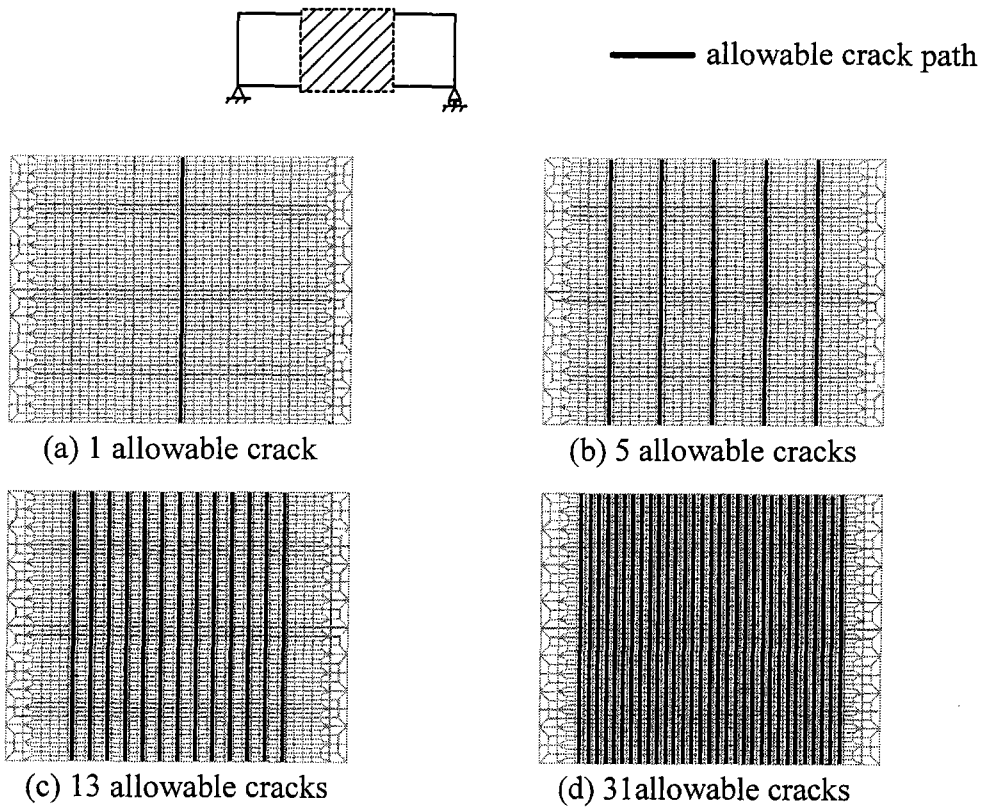

Fig. 7.6 Specimen with different numbers of allowable crack paths

Table 7.1 GA parameters

Population size	40
Number of generations	40
Crossover probability	0.80
Mutation probability	0.05

paths. The problem is solved both with and without the specimen's self-weight. When the self-weight is neglected, the problem is solved with various numbers of allowable crack paths as shown in Fig. 7.6, and, in all of these cases with different allowable crack paths, the equilibrium path with the minimum total potential energy increment is traced by employing an exhaustive search. In addition, only for the case with 31 allowable crack paths, a GA is also employed for the search. When the self-weight is considered, the analysis is done only for the case with 31 allowable crack paths, and the equilibrium path with the minimum total potential energy increment is traced by employing both exhaustive search and GA. GA parameters used in the analysis are shown in Table 7.1. Note that, in those cases where the GA is used for the search, it will be used when there are more than 10 cracks occurring in the specimen because the advantages of the genetic algorithm are not significant in small search space.

Fig. 7.7a shows load-controlled displacement responses for all of the calculations mentioned above. Moreover, it also includes the case with 31 allowable

crack paths when the cracking localization is not considered. This additional case is performed without the self-weight and it will allow the importance of the localization analysis to be observed. Fig. 7.7b shows crack patterns obtained from these different cases at the loading points indicated by black circular markers on every response curve. At these loading points, the main cracks in all cases reach the length of 90 percent of the beam depth. For the case with 31 allowable crack paths with the localization consideration (the cases D and E), it can be seen that the results obtained from the exhaustive search and the GA are exactly the same. Therefore, it is shown that GAs can be used instead of the exhaustive search. It must be noted that the time used by the exhaustive search is very much longer than that used by the GA. For the cases B, C, and D where no self-weight is assumed, it can be seen that the obtained results, both crack patterns and response curves, are not much different. Therefore, for this problem, having only five allowable crack paths that are distributed properly is sufficient for obtaining the converged solution. Since it can be observed from the crack patterns of the cases B, C, and D that there are actually two long cracks in the beam, it may be understood that the response is actually governed by two main localized cracks which are not localized into one crack until at a much later loading stage. Also from the response curves, it is seen that the results of the case A, which assumes one localized crack at the center of the span, and the case F, which does not consider the localization, are very much different from those of the cases B, C, and D which properly consider the localization. Finally, from a comparison of the results of the cases D (without self-weight) and E (with self-weight), it can be seen that the load-displacement responses of both cases are very similar. Therefore, for this particular problem, neglecting the self-weight does not have a significant effect. Nevertheless, it can also be observed from the obtained crack patterns that the two main cracks are closer to each other when the self-weight is considered. This is expected since the self-weight makes the stress higher at locations closer to the center of the span. Fig. 7.8 shows the crack patterns of the cases D and E at different loading stages.

The results obtained from this problem clearly show that the true localized solutions are very much different from the solution obtained by assuming one localized crack at the center of the span. Furthermore, the true localized solutions are also very much different from the solution obtained without the localization consideration. It is also found that there are two major localized cracks that are not localized into one crack until at a much later loading stage. The behavior of the beam is therefore governed by these two cracks. This clearly illustrates that assuming only one localized crack from the beginning may lead to erroneous results. Finally, it is found that, for the four-point bending test of plain concrete, neglecting the self-weight does not have significant effect on the obtained results. With self-weight or without self-weight, there are two main localized cracks. Although these two cracks are slightly closer when the self-weight is considered, the difference between the obtained responses from both cases is negligible.

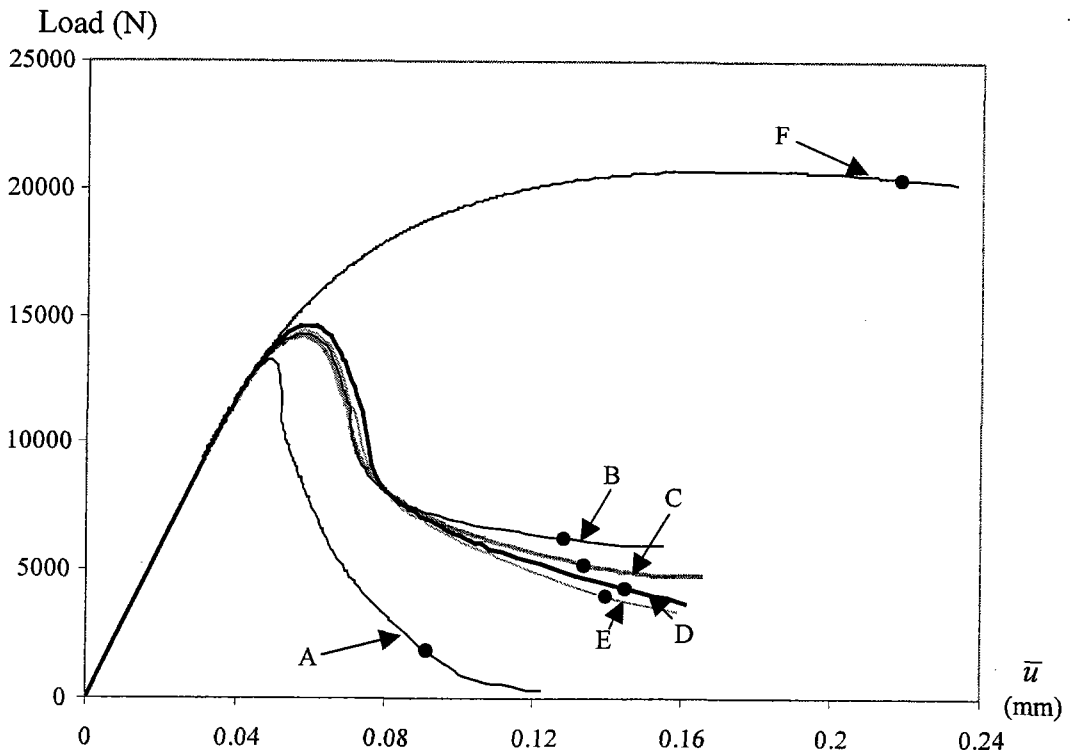

(a) Load-controlled displacement responses

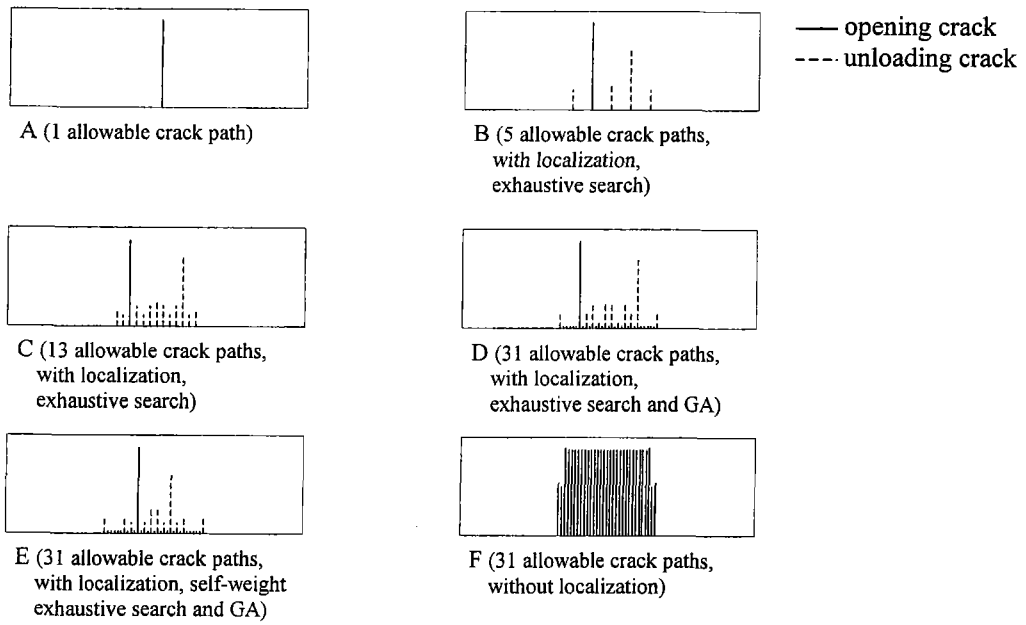

(b) Crack patterns

Fig. 7.7 Load-controlled displacement responses and crack patterns

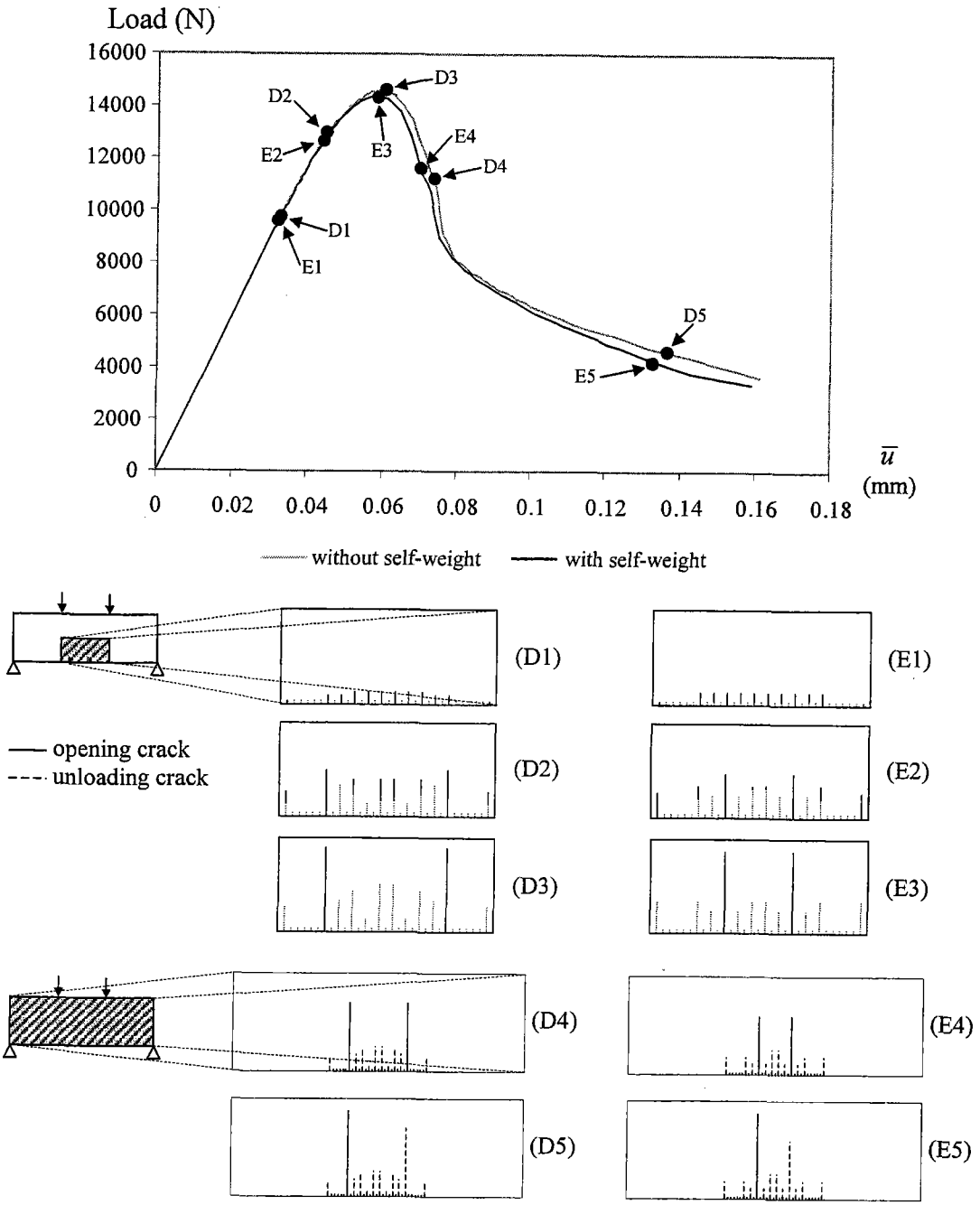

Fig. 7.8 Crack patterns of specimen with 31 allowable crack paths

7.3 A Four-Point Bending Problem of Steel-Fiber-Reinforced Concrete Using Four-Noded Quadrilateral Elements

This test is the same as the previous one but the material used is changed from plain concrete to steel-fiber-reinforced concrete. Different responses from those responses of the previous example are expected because steel-fiber-reinforced concrete has much larger fracture energy than plain concrete due to the presence of its steel fibers. The steel fibers will help transmit the bridging stresses across the cracks. They will make the stress transmission possible even when the crack opening displacement becomes large. This fact will be automatically incorporated into the calculation by means of the tension-softening curve. The tension-softening curve of steel-fiber-reinforced concrete will have a longer tail and larger area under the curve than the curve for plain concrete. The area under a tension-softening curve represents the fracture energy of the material.

The dimensions of the specimen and its boundary conditions are exactly the same as those of the previous example. Young's modulus and Poison's ratio used are 36.3 GPa and 0.2, respectively. Unit weight of the material is 2,500 kg/m^3. The tension-softening curve used is shown in Fig. 7.9b. The finite element mesh in Fig. 7.5 is also used in this problem.

For this problem, it is still assumed that all crack paths are straight and cracks will be allowed to occur only on the pre-specified paths which are shown in Fig. 7.10. When the case with one allowable crack path is considered, it implies that the cracking localization is neglected. For the case with 31 allowable crack paths, the equilibrium path with the minimum total potential energy increment is traced by

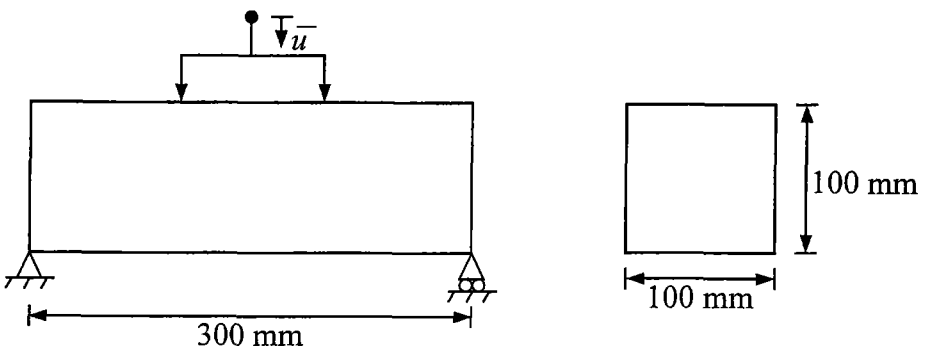

(a) Specimen geometry

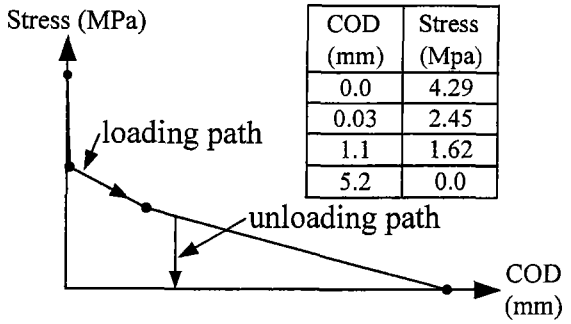

COD (mm)	Stress (Mpa)
0.0	4.29
0.03	2.45
1.1	1.62
5.2	0.0

(b) Tension-softening curve

Young's Modulus = 36,300 MPa
Poison's Ratio = 0.2

(c) Elastic properties

Fig. 7.9 Four-point bending problem of steel-fiber-reinforced concrete

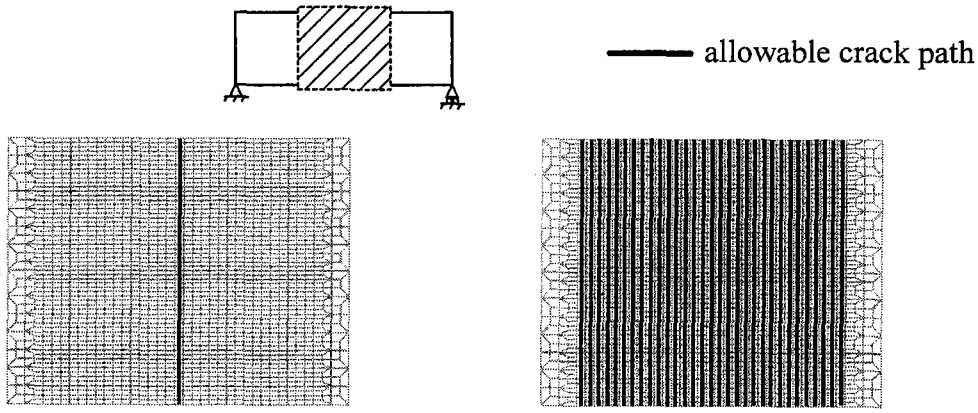

(a) 1 allowable crack (b) 31 allowable cracks

Fig. 7.10 Specimen with different numbers of allowable crack paths

employing both the exhaustive search and GA. Note that, similar to the previous problem, the genetic algorithm will be used only when there are more than 10 cracks occurring in the specimen. GA parameters used in the analysis are shown in Table 7.1. For both cases, the problem is solved with the specimen's self-weight.

Fig. 7.11a shows load-controlled displacement responses of the two cases. In the figure, case A represents the case when one crack is assumed from the beginning (see Fig. 7.10a). In addition, case B represents the case when 31 crack paths are allowed (see Fig. 7.10b). Crack patterns obtained from both cases are shown in Fig. 7.11b. The corresponding loading points are indicated by black circular markers on the response curves. At these stages, the length of the main cracks in all cases reach 80 percent of the beam depth and the analyses are stopped. This is because the compressive stress in the ligaments becomes high and the nonlinear material behavior in compression can no longer be neglected. Note that nonlinear material behavior is not considered in this study.

From the obtained response curves, it can be seen that the post-peak response obtained with proper localization consideration is quite different from the one with pre-assumed crack at the center of the span. Assuming one crack from the beginning results in somewhat more brittle behavior. This is logical since having one crack from the beginning implies that the cracks are forced to localize into one crack from the beginning. From the crack patterns, it is clear that there are two major cracks in the case with the consideration of cracking localization. These two cracks are expected to localize into one crack if the loading continues. Therefore, if only one crack is assumed from the beginning, it is obvious that the analysis done in such a fashion will not be able to capture this localization behavior.

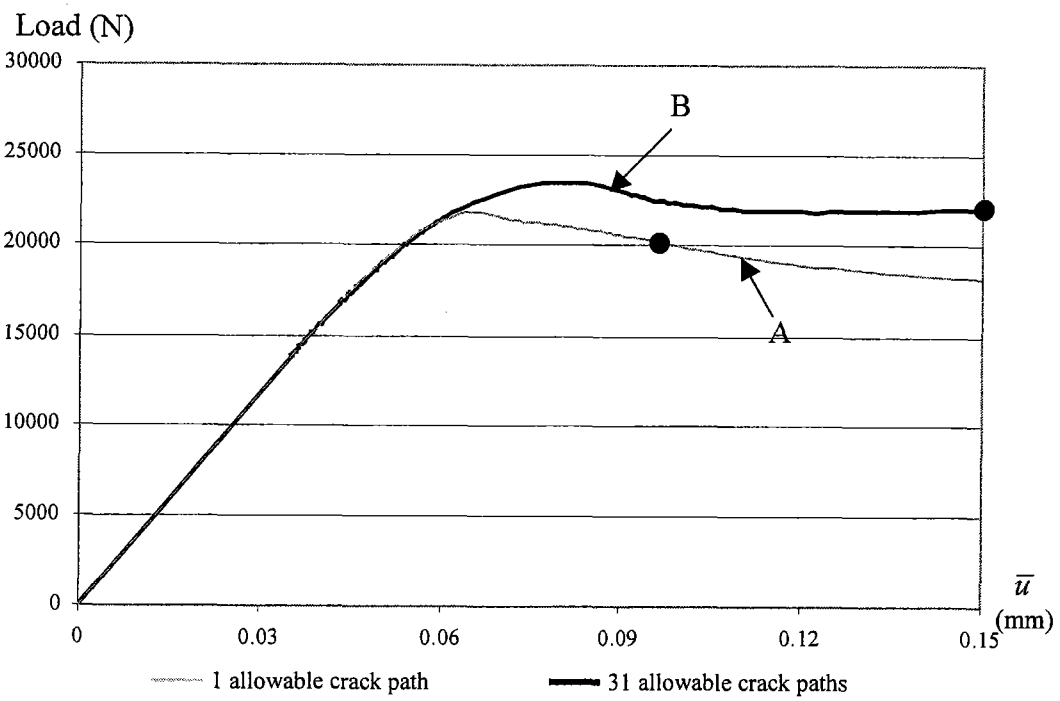

(a) Load-controlled displacement responses

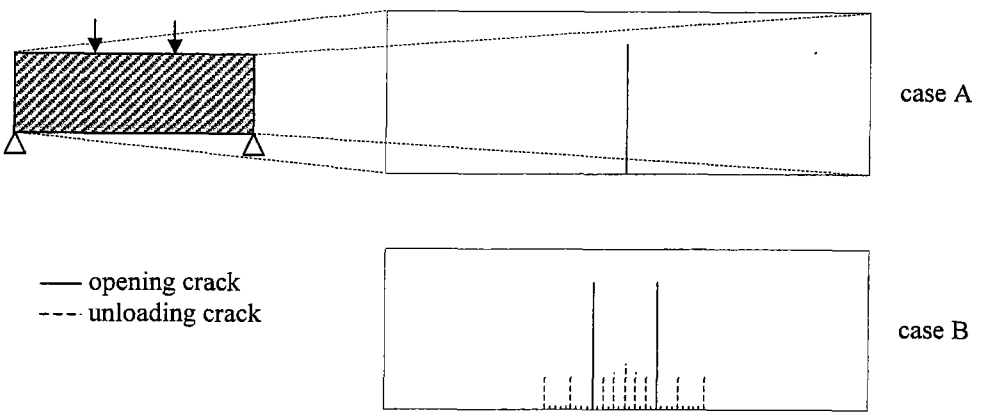

(b) Crack patterns

Fig. 7.11 Load-controlled displacement responses and crack patterns